Inhibition of the SHV-1 β-Lactamase by Sulfones: Crystallographic Observation of Two Reaction Intermediates with Tazobactam[†,‡]

Alexandre P. Kuzin,[§] Michiyoshi Nukaga,[§] Yasuko Nukaga,[§] Andrea Hujer,[||] Robert A. Bonomo,[||] and James R. Knox*[,§]

Department of Molecular and Cell Biology, The University of Connecticut, Storrs, Connecticut 06269-3125, and Research Service, Department of Veterans Affairs Medical Center, Cleveland, Ohio 44106

Received September 27, 2000; Revised Manuscript Received November 17, 2000

ABSTRACT: Two species resulting from the reaction of the SHV-1 class A β-lactamase with the sulfone inhibitor tazobactam have been trapped at 100 K and mapped by X-ray crystallography at 2.0 Å resolution. An acyclic form of tazobactam is covalently bonded to the catalytic Ser70 side chain, and a second species, a five-atom vinyl carboxylic acid fragment of tazobactam, is bonded to Ser130. It is proposed that the electron density map of the crystal is a *composite* picture of two complexes, each with only a single bound species. It is estimated that the two complexes exist in the crystal in approximately equal populations. Results are discussed in relation to the mechanism-based inhibition of class A β-lactamases by the similar inhibitors sulbactam and clavulanic acid.

Bacterial β-lactamases provide resistance to β-lactams (penicillins, cephalosporins, monobactams, carbapenems) by hydrolyzing the β-lactam bond (*1*−*4*). Two major groups of β-lactamases have been identified and are catalytically distinguished by the employment of either a reactive serine residue (in classes A, C, and D) or a zinc center (in class B) (*5*). The clinically important SHV-1 and TEM-1 β-lactamases are serine enzymes of class A, and they are the prototypes from which numerous spontaneous mutants have arisen in response to the use of modern β-lactams (*6*, *7*). Beginning in the late 1980s, three β-lactamase inhibitors, tazobactam (**1**), sulbactam, and clavulanic acid, have been used against the serine enzymes, usually in combination with penicillins more susceptible to β-lactamase hydrolysis (*8*−*10*). This therapeutic strategy has been effective for a decade, but SHV and TEM mutants recently discovered have significant resistance to these mechanism-based inhibitors (*11*−*14*).

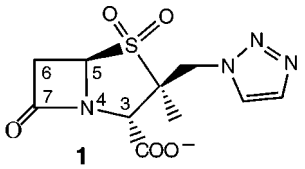

1

Tazobactam is a triazolyl-substituted penicillanic acid sulfone which is often used in combination with piperacillin, a broad spectrum penicillin (*15*). The inhibitor is effective against class A β-lactamases and some class C β-lactamases. In its reactions with these enzymes, it first acylates the reactive serine and then partitions between a hydrolysis pathway and an inactivation pathway involving interaction with other nucleophiles and resulting in irreversible inhibition. For some β-lactamases, hundreds or thousands of hydrolytic turnovers are required until inhibition is achieved (*16*).

From early spectroscopic and kinetic studies (*16*, *17*), modeling and molecular dynamics calculations (*18*, *19*), crystallography (*20*), and mass spectroscopy (*15*, *21*), as many as 8−10 intermediates have been proposed to exist along the hydrolysis and inactivation pathways of these inhibitors with the class A enzymes. We report here cryocrystallographic experiments to isolate tazobactam reaction intermediates with the SHV-1 β-lactamase at pH 7. By establishing how tazobactam makes use of the stereochemistry of the class A binding site, modifications of the inhibitor might become apparent in order to optimize its partitioning in favor of inactivation.

MATERIALS AND METHODS

Enzyme Preparation. The enzyme was expressed and purified as previously described (*22*). The SHV-1 β-lactamase gene (bla_{SHV-1}, GenBank accession no. AF124984) had been directionally subcloned into the phagemid vector pBCSK (Stratagene, La Jolla, CA) from a clinical strain of *Klebsiella pneumoniae* 15571. *Escherichia coli* DH10B [F$^-$ *mcr*A Δ(*mrr-hsd*RMS-*mcr*BC) ϕ80d*lac*ZDM15 Δ*lac*X74 *deo*R *rec*A1 *end*A1 *ara*D139 Δ(*ara*, *leu*)7697*gal*U *gal*K λ^- *rps*L *nup*G] was the host strain used to harvest the SHV-1 enzyme (Gibco BRL, Grand Island, NY).

Crystallization. Native crystals measuring up to 0.25 mm in all dimensions were grown at room temperature by the vapor diffusion method. The protein drop [2 mg/mL, 0.56

[†] This work was supported by grants from the Department of Veterans Affairs and Wyeth-Ayerst Research to R.A.B. and J.R.K. and from the National Institute of Aging (NIH/NIA AG-00634) to R.A.B.

[‡] Atomic coordinates have been deposited in the Protein Data Bank (entry 1G56) at Rutgers University.

* Corresponding author: phone 860-486-3133; fax 860-486-4745; e-mail knox@uconnvm.uconn.edu.

[§] The University of Connecticut.

[||] Department of Veterans Affairs Medical Center.

10.1021/bi0022745 CCC: $20.00
Published on Web 01/11/2001

Table 1: Tazobactam Reaction Conditions

data set	final concn (mM)	crystal soak time (h at 20 °C)	appearance of electron density map
1	42	3	no excess density in catalytic site
2	42	6	density extending from Ser70 and Ser130
3	1	28	similar to data set 1
4	42	96	density extending from Ser130 only

mM Cymal-6[1] detergent (Anatrace, Maume, OH), 15% PEG (M_r = 6000, Hampton Research, Lagnua Niguel, CA), 50 mM HEPES buffer, pH 7.0] was placed over a reservoir solution containing 30% PEG and 100 mM HEPES buffer. The enzyme crystallizes in space group $P2_12_12_1$ with a = 49.6 Å, b = 55.6 Å, and c = 87.0 Å (293 K) and one molecule in the asymmetric unit (*22*).

Preparation of Tazobactam Complexes. Tazobactam (99.5% pure) was a gift of Wyeth-Ayerst Research (Pearl River, NY). Pregrown native crystals of SHV-1 were soaked at room temperature in the 30% PEG holding solution (pH 7) containing Cymal-6 and tazobactam, the concentration of which was incrementally increased over several hours to minimize cracking. Four experiments to optimize complexation were made using crystal soaking times ranging up to 96 h and tazobactam concentrations up to the solubility limit (Table 1). In each experiment the tazobactam solution was refreshed 30 min before crystal freezing and X-ray data collection.

X-ray Data Collection. Crystals were loop-mounted and dipped for 1−2 min in the cryoprotected PEG holding solution containing tazobactam and 25% MPD before flash freezing in a gaseous nitrogen stream (Oxford Cryosystems). Data were collected at 100 K on a Bruker HISTAR multiwire area detector on a Rigaku RU-200 rotating anode generator operating at 40 kV and 60 mA with a 3 mm filament (Cu Kα radiation) and double-mirror Franks focusing. At a detector distance of 10 cm, 1024 × 1024 pixel frames were counted for 180 s through an omega step of 0.25°. Intensities were indexed and scaled with XGEN (Molecular Simulations, Inc.).

RESULTS

Optimization of Reaction Conditions. In searching for conditions producing maximum difference electron density in the catalytic site, it was necessary to calculate maps from four data sets from crystals soaked in a range of concentrations of tazobactam for time periods of 3−96 h (Table 1). Soaking for 6 h in 42 mM tazobactam (data set 2) produced a promising map; for these data R_{sym} = 0.077 for 14 910 unique reflections from 69 096 observations for an overall completeness of 95% (Table 2). Cell dimensions for the complex are 49.2 Å × 56.1 Å × 82.5 Å (100 K), the c dimension being shorter by 5% than the native cell dimension at 293 K. The large change in the cell dimension is probably due to the temperature difference rather than tazobactam binding, because two other soaked crystals (data sets 1 and 3), not showing tazobactam binding, also had a shortened c cell dimension at 100 K.

[1] Abbreviations: Cymal-6, cyclohexyl-(*n*-hexyl) β-D-maltoside; MPD, 2-methyl-2,4-pentanediol; PEG, poly(ethylene glycol); rmsd, root of the mean squared deviations.

Table 2: X-ray Data Collection for Data Set 2[a]

temp (K)	100
d_{min} (Å)	2.02 (2.14−2.02)
observations	69096 (4543)
unique reflections	14910 (1843)
completeness	0.95 (0.72)
av $I/\sigma(I)$	12.1 (2.5)
$R_{sym}(I)$[b]	0.077 (0.26)

[a] Data for highest resolution shell are in parentheses. [b] $R_{sym} = \sum|I_{av} - I_i|/\sum I_i$, where I_{av} is the average of all individual observations, I_i. The space group is $P2_12_12_1$.

Structure Determination. The four crystal structures were solved by molecular replacement with the program AMoRe (*23*) using the structure of the native SHV-1 β-lactamase [1SHV, Protein Data Bank (*22*)]. Because of significant differences in cell constants between complex and native crystals, it was necessary to use rigid body refinement in X-PLOR (*24*). Data set 2 provided the most readily interpretable map, and this was the only structure subjected to full refinement.

Electron Density in the Catalytic Site. In the map from data set 2, tazobactam moieties were seen covalently bound to the Oγ atom of two serine residues in the catalytic site (Figure 1a). First, a linear form of tazobactam, in which both the β-lactam and sulfone rings are open, binds to Ser70. Dihedral angles rather than bond distances were used to help to distinguish between the imine and enamine forms of the linear species (**3**, **4**, and **5**, Figure 2). The unrestrained refinement (see below) produced dihedral angles about the N4−C5 and C5−C6 bonds equal to 144° and 113°, respectively, and the imine structure **3** was assigned to the Ser70 intermediate. There is no indication of the coexistence of multiple conformers of **3**, as seen in the map of a clavulanate intermediate bound to the PC1 β-lactamase (*20*). A peak at the 3σ level in the difference map near C6 indicates the possible existence of a shorter aldehyde species **10** or **11** overlaying the primary species **3**. Due to uncertainty, species **10** and **11** were not included in the model, however. Quite clear is a five-atom vinyl carboxylic acid fragment **9** bound to Ser130. The conformation about the vinyl C−C bond is trans (dihedral angle = 177°). This Ser130 moiety is better fit to the map than the Ser70 moiety, which displays some disorder beyond the C3 atom. A qualitative description of the electron density under other reaction conditions is given in Table 1.

Intermolecular Electron Density. A region of connected electron density above the 3σ level was observed between neighboring molecules, and it persisted to the final stages of refinement of data set 2. The size of the density was incompatible with solvent, cryoprotectant, buffer, or Cymal-6 detergent (which had been found to bind elsewhere). All of the density could be fit with the structure of unreacted tazobactam (Figure 1b). Given the high initial concentration of tazobactam (42 mM), it is perhaps not unusual that we observe the immobilization of the inhibitor near the edge of the catalytic site (Figure 3).

Structure Refinement. Mild simulated annealing refinement was done at 500 and 300 K with X-PLOR (*24*), followed by side-chain torsion angle refinement and *B*-factor refinements.

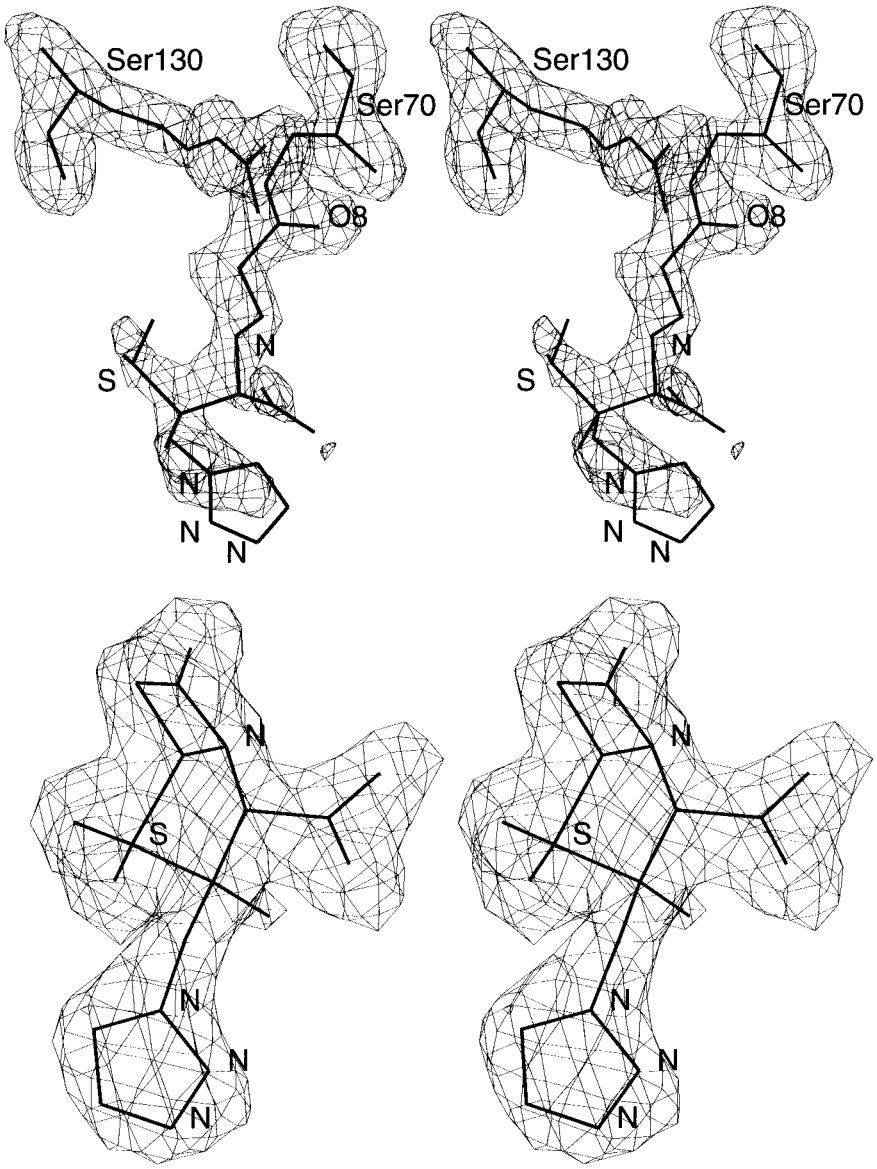

FIGURE 1: Stereoviews of $F_o - F_c$ electron densities as plotted by CHAIN (*25*) with all tazobactam species omitted from the F_c calculation. (a, top) The acyclic intermediate bound to Ser70 (species **3**) and the vinyl carboxylic acid fragment bound to Ser130 (**9**). The contour level is 2.4σ. (b, bottom) The surface-bound unreacted molecule of tazobactam with a contour level of 2σ.

A bulk solvent correction was included. Maps using all data from 20 to 2 Å were calculated, and rounds of manual fitting using the programs CHAIN (*25*) and FRODO (*26*) were done to optimize backbone and side-chain conformations. Significant difference density in the catalytic site was left unmodeled until the *R*-factor approached 0.25. A final refinement using anisotropic scaling and the maximum-likelihood method in REFMAC (*27*) included tazobactam moieties bound to Ser70 and Ser130 (each assigned 0.5 occupancy, but see Disscussion), a noncovalently bound molecule of tazobactam (occupancy 1.0), all 265 amino acid residues, one Cymal-6 detergent molecule (occupancy 0.25), the cyclohexyl ring of a disordered Cymal-6 molecule, and 175 water molecules (with *B*-factors < 60 Å^2). Initial bond and angle parameters for the tazobactam moieties were obtained from the crystal structure of tazobactam (*28*). Torsion angles for the tazobactam moieties were unrestrained during refinement. The resulting crystallographic *R*-factor is 0.177 for data with $F > 0\sigma(F)$ in the range 50−2 Å (Table 3). The R_{free} value is 0.257 (*29*). In the Ramachandran plot 92.2% of the residues are in favored regions and none are in disallowed regions. Atomic coordinates from data set 2 have been deposited in the Protein Data Bank (Entry 1G56) at Rutgers University.

DISCUSSION

The Ser70-bound moiety (**2**) is thought to be the initial intermediate of the multistep inhibitory process employed by mechanism-based inhibitors such as sulfones and clavulanate (Figure 2) (*15*, *17*−*21*). Ring opening after departure of the sulfinate from C5 produces a reactive imine (**3**) and the more inert tautomeric enamine forms (**4**, **5**). Intermediate **3** can undergo hydrolysis, either directly or via species **10** and **11**, to regenerate the active enzyme. Less frequent reaction of **3** with an active site nucleophile, either a lysyl amine (*17*) or a serine hydroxyl group (*18*, *19*), had been proposed to lead to irreversible inhibition. The nature of the species in the reaction pathway was not clear. To identify the nucleophile and reaction intermediates and/or products, mass spectroscopy studies under nonphysiological conditions,

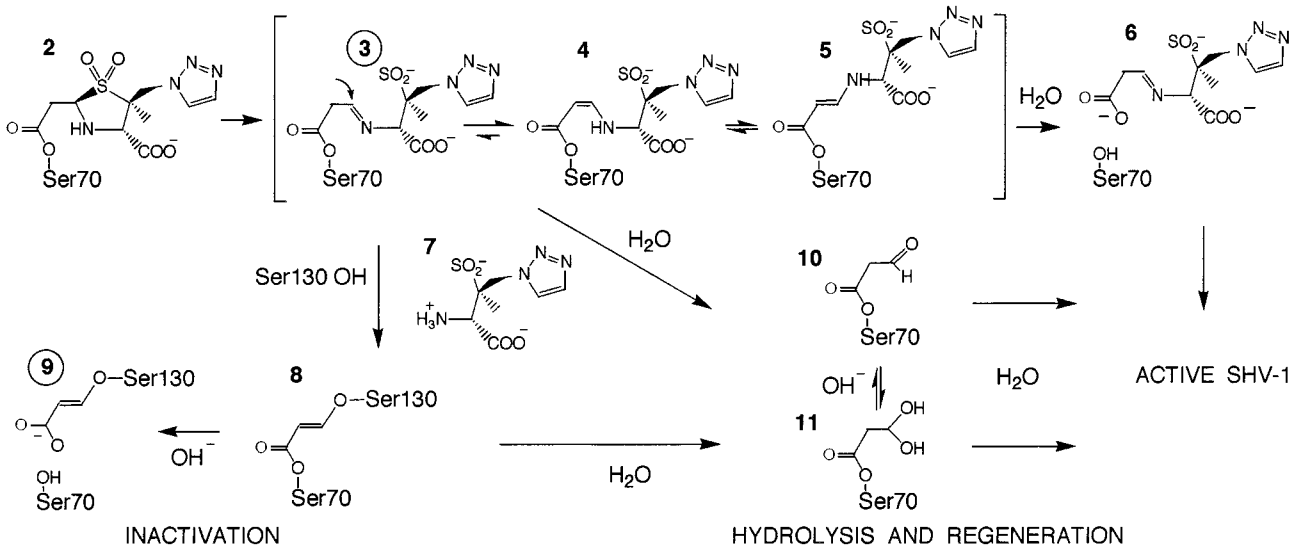

FIGURE 2: Proposed reaction mechanism of tazobactam with the SHV-1 β-lactamase. Circled species are assigned to electron densities observed in this study. The scheme is adapted from refs *15*, *17*, *19*, and *21*.

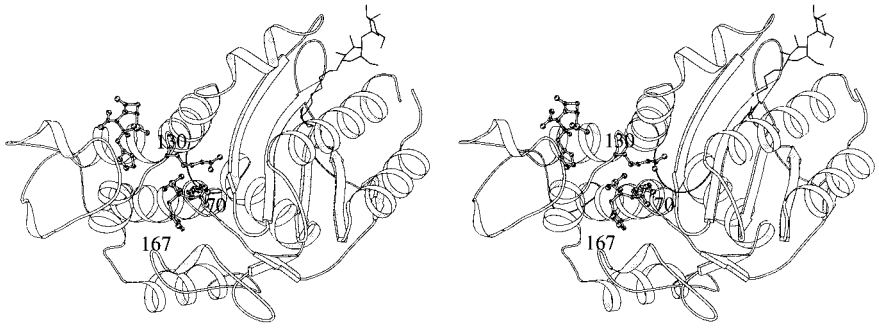

FIGURE 3: Stereoview of the SHV-1 β-lactamase with the tazobactam reaction species bound to Ser70 and Ser130. The unreacted surface-bound tazobactam is shown near residues 104−106. A molecule of the detergent Cymal-6 is bound near the C-terminal helix. The figure is drawn by MOLSCRIPT (*34*).

Table 3: Crystallographic Refinement

resolution range (Å)	50−2.0
no. of reflections used [$F > 0\sigma(F)$]	13813
R-factor	0.177
R_{free}-factor	0.257
Ramachandran zones (%)	
favored	92.2
allowed	7.8
disallowed	0.0
rms deviations from ideality	
bond lengths (Å)	0.016
bond angles (deg)	2.3
planarity (Å)	
peptide groups	0.025
aromatic groups	0.015
mean *B*-factors (Å^2)	
protein	13.8
Ser70 intermediate	28.9
Ser130 intermediate	29.0
surface-bound tazobactam	21.2
water molecules	26.2
all atoms	15.2

first for the reaction of clavulanate with the TEM β-lactamase (*21*) and lately for tazobactam with the PC1 enzyme (*15*), have now been joined by our cryocrystallography on a catalytically active β-lactamase crystal at pH 7. Taken together, these experiments confirm the reaction of a nucleophilic Ser130 with imine **3**. Following the displacement of the sulfinic acid fragment (**7**), the bridging species **8** is expected to form (*17*). Subsequent hydrolysis at the Ser70 end of the bridge produces a Ser130-bound carboxylic acid moiety **9**, the second of two intermediates observed in this study, and the probable terminal species from the tazobactam reaction.

The Ser70 Intermediate. Given the observed dihedral angles about N4−C5 and C5−C6, we have assigned structure **3** to the moiety on Ser70 (Figure 4). The carbonyl group of the opened β-lactam ring is hydrogen bonded between NH69 and NH237 in an oxyanion hole. The sulfinic acid group of **3** hydrogen bonds to the side-chain amide of Asn132, but the carboxylic acid group has no hydrogen bonds to the enzyme. The triazolyl ring contacts Thr167 and Asn170 on the omega loop at the bottom of the catalytic site. The probable hydrolytic water molecule (W636) is seen below the acyl ester bond, hydrogen bonded between Glu166 and Asn170, as in the native structure (*22*). Given the composite nature of the electron density map (see below), we cannot say whether this water molecule is associated with the Ser70 intermediate or the Ser130 species or both.

The Ser130 Species. Following the early hypotheses of Knowles (*17*), simulations for clavulanate and sulbactam inhibition (*18*, *19*) confirmed that moderate dynamics would allow the reactive intermediate **3** to come near hydroxyl and amine nucleophiles in the binding site of the class A β-lactamase. Our results with tazobactam identify this enzymic agent as Ser130, the hydroxyl group of which

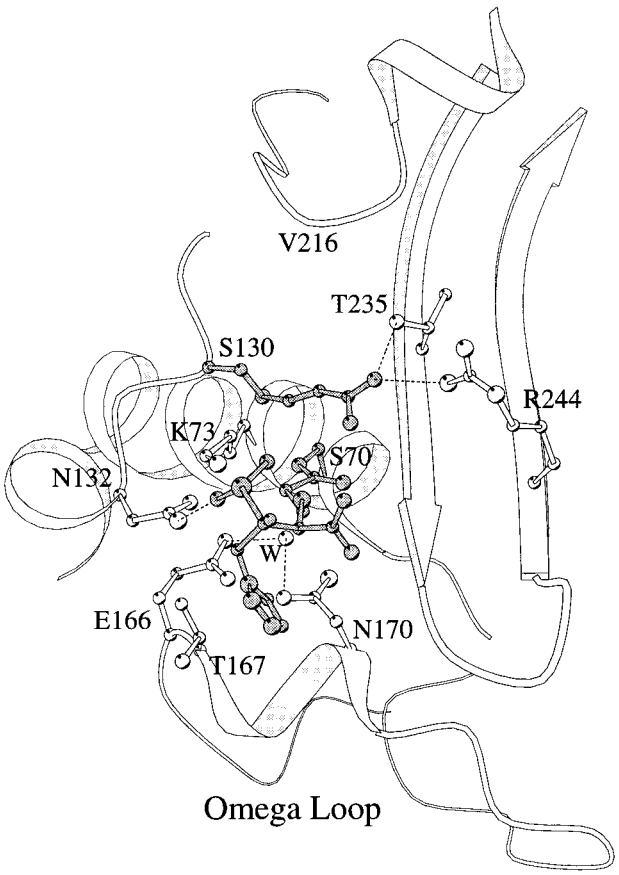

FIGURE 4: Environment of the tazobactam species bound to Ser70 and Ser130 in the catalytic site of SHV-1. The probable hydrolytic water molecule (W636) is indicated by W. The figure is drawn by MOLSCRIPT (*34*).

attacks the C5 atom of intermediate **3**. Reaction of **3** with Ser130 directs partitioning in favor of irreversible inactivation. Here we note that the inhibitory superiority of tazobactam over sulbactam (*8*, *16*, *30*), which lacks the triazolyl ring, may be due in part to the fact that steric contact of the triazolyl ring with Thr167 and Asn170 at the bottom of the binding site restricts the motion of **3** to the upper part of the binding site, where it is more likely to encounter the hydroxyl group of Ser130.

Attack by Ser130 produces the leaving fragment **7** and forms a bridging species **8**. Hydrolysis at the Ser70 end of **8** results in the five-atom vinyl carboxylic acid species **9** (Figure 4). Species **9** is well ordered in the catalytic site, hydrogen bonding with the hydroxyl group of Thr235 (3.0 Å) and with the guanidinium group of Arg244 (3.1 Å). Crystallographic experiments under four reaction conditions (Table 1) did not detect bridging intermediate **8**, demonstrating its instability at pH 7. Two pathways for the breakdown of an equivalent bridging species in clavulanate inhibition have been discussed (*21*). One path results in the Ser130 moiety we find with tazobactam, while another path proceeds via Ser70-bound aldehyde/hydrate intermediates (**10**, **11**) to regenerate the active enzyme. Conceivably, low populations of smaller intermediates **10** or **11** could be present in the space of the larger **3** but would be unresolved from **3** in our mapping at this resolution.

For several reasons we believe that the Ser130 moiety **9** is the terminal species in the inhibition reaction with tazobactam. First, data from a crystal soaked in the inhibitor for a longer time and with the highest concentration (data set 4, Table 1) resulted in a map having no excess density on Ser70, only on Ser130. Second, from a steric standpoint, the moiety on Ser130 would prevent entry and alignment of another molecule of tazobactam. Third, from a chemical standpoint, this modification of Ser130 by tazobactam would obviously prevent participation of the hydroxyl group of Ser130 in subsequent β-lactam binding (*31*) or catalytic turnover (*2*, *32*, *33*). Therefore, we think that only a single tazobactam species, *either* **3** or **9**, is covalently bound to a given molecule of the enzyme. From our electron density map we estimate that approximately half the molecules in the crystal are fully labeled with **3** and the other half with **9**. In this case, the map of the crystal (Figure 1a) is a *composite* picture of two complexes, falsely indicating that the two reaction species occur together in the catalytic site. Fortunately, it permits us to observe two intermediates of the reaction. Allowing the reaction to go for a longer time labels all molecules in the lattice at Ser130 only (Table 1, data set 4).

A combination of X-ray crystallography and mass spectroscopy has firmly established a central role for Ser130 in the inhibition of class A β-lactamases by tazobactam and clavulanic acid. It can now be appreciated why inhibitor-resistant mutants of the SHV and TEM enzymes have been found with glycine replacing serine at position 130 (*11*, *13*). These natural mutants will not form the terminal tazobactam species **9**, and they maintain the more important ability to hydrolyze β-lactam antibiotics via Ser70, whose interaction with tazobactam is only transient. Catalytically, the Ser130Gly mutant is a poorer β-lactamase, but it successfully avoids inactivation by multisite inhibitors such as tazobactam.

ACKNOWLEDGMENT

We thank Drs. Youjun Yang and David Shlaes (Wyeth-Ayerst Research) for an unpublished manuscript.

REFERENCES

1. Massova, I., and Mobashery, S. (1997) *Acc. Chem. Res. 30*, 162−168.
2. Matagne, A., Lamotte-Brasseur, J., and Frere, J.-M. (1998) *Biochem. J. 330*, 581−598.
3. Bush, K., and Mobashery, S. (1998) in *Resolving the Antibiotic Paradox* (Rosen, B., and Mobashery, S., Eds.) pp 71−98, Kluwer Academic/Plenum Publishers, New York, NY.
4. Kotra, L. P., and Mobashery, S. (1998) *Bull. Inst. Pasteur 96*, 139−150.
5. Page, M. I., and Laws, A. P. (1998) *Chem. Commun.*, 1609−1617.
6. Knox, J. R. (1995) *Antimicrob. Agents Chemother. 39*, 2593−2601.
7. Bush, K., and Jacoby, G. (1997) *J. Antimicrob. Chemother. 39*, 1−3.
8. Payne, D. J., Cramp, R., Winstanley, D. J., and Knowles, D. J. C. (1994) *Antimicrob. Agents Chemother. 38*, 767−772.
9. Yang, Y., Rasmussen, B. A., and Shlaes, D. M. (1999) *Pharmacol. Ther. 83*, 141−151.
10. Page, M. G. P. (2000) *Drug Resist. Updates 3*, 109−125.
11. Prinarakis, E. E., Miriagou, V., Tzelepi, E., Gazouli, M., and Tzouvelekis, L. S. (1997) *Antimicrob. Agents Chemother. 41*, 838−840.
12. Lin, S., Thomas, M., Shlaes, D. M., Rudin, S. D., Knox, J. R., Anderson, V., and Bonomo, R. A. (1998) *Biochem. J. 333*, 395−400.

13. Bermudes, H., Jude, F., Chaibi, E. B., Arpin, C., Bebear, C., Labia, R., and Quentin, C. (1999) *Antimicrob. Agents Chemother. 43*, 1657−1661.
14. Chaibi, E. B., Sirot, D., Paul, G., and Labia, R. (1999) *J. Antimicrob. Chemother. 43*, 447−458.
15. Yang, Y., Janota, K., Tabei, K., Huang, N., Siegel, M. M., Lin, Y.-I., Rasmussen, B. A., and Shlaes, D. M. (2000) *J. Biol. Chem. 275*, 26674−26682.
16. Bush, K., Macalintal, C., Rasmussen, B. A., Lee, V. J., and Yang, Y. (1993) *Antimicrob. Agents Chemother. 37*, 851−858.
17. Knowles, J. R. (1985) *Acc. Chem. Res. 18*, 97−104.
18. Imtiaz, U., Billings, E. M., Knox, J. R., Manavathu, E. K., Lerner, S. A., and Mobashery, S. (1993) *J. Am. Chem. Soc. 115*, 4435−4442.
19. Imtiaz, U., Billings, E. M., Knox, J. R., and Mobashery, S. (1994) *Biochemistry 33*, 5728−5738.
20. Chen, C. C. H., and Herzberg, O. (1992) *J. Mol. Biol. 224*, 1103−1113.
21. Brown, R. P. A., Aplin, R. T., and Schofield, C. J. (1996) *Biochemistry 35*, 12421−12432.
22. Kuzin, A. P., Nukaga, M., Nukaga, Y., Hujer, A. M., Bonomo, R. A., and Knox, J. R. (1999) *Biochemistry 38*, 5720−5727.
23. Navaza, J. (1994) *Acta Crystallogr. A50*, 157−163.
24. Brunger, A. T. (1992) *X-PLOR: A system for X-ray crystallography and NMR*, Yale University Press, New Haven, CT.
25. Sack, J. S. (1988) *J. Mol. Graphics 6*, 224−225.
26. Jones, T. A. (1985) *Methods Enzymol. 115*, 157−170.
27. Murshudov, G. N., Vagin, A. A., and Dodson, E. J. (1997) *Acta Crystallogr. D53*, 240−255.
28. Toomer, C. A., Schwalbe, C. H., Ringan, N. S., Lambert, P. A., Lowe, P. R., and Lee, V. L. (1991) *J. Med. Chem. 34*, 1944−1947.
29. Brunger, A. T. (1992) *Nature 355*, 472−475.
30. Swaren, P., Golemi, D., Cabantous, S., Bulychev, A., Maveyraud, L., Mobashery, S., and Samama, J.-P. (1999) *Biochemistry 38*, 9570−9576.
31. Juteau, J.-M., Billings, E. M., Knox, J. R., and Levesque, R. C. (1992) *Protein Eng. 5*, 693−701.
32. Ishiguro, M., and Imajo, S. (1996) *J. Med. Chem. 39*, 2207−2218.
33. Damblon, C., Raquet, X., Lian, L.-Y., Lamotte-Brasseur, J., Fonze, E., Charlier, P., Roberts, G. C. K., and Frere, J.-M. (1996) *Proc. Natl. Acad. Sci. U.S.A. 93*, 1747−1752.
34. Kraulis, P. (1991) *J. Appl. Crystallogr. 24*, 946−950.

BI0022745